Nowhere to hide: identifying AGN in the faint radio sky

Radcliffe, Jack Frederick

7

Future prospects

While this thesis has begun to answer some questions regarding the radio-faint AGN population, this chapter aims to outline some of the issues we aim to tackle with the completion of the GOODS-N project, the upcoming deep EVN-COSMOS project and surveys using MeerKAT and SKA-VLBI.

7.1. Extending multi-source self-calibration: CASA and direction dependent calibration

With the addition of the fringe-fitting capabilities to CASA v. 5.3 (released 06/2018), VLBI data can now be reduced using this up-to-date software package. In light of this, the MSSC calibration code that was originally written for the AIPS calibration package will need to be rewritten in CASA in order to maintain its usefulness in future observations.

Initial steps have been made in order to port the MSSC algorithm into a CASA task and we shall aim to release this in an upcoming CASA release.* The parallelisation capabilities provided by CASA should improve the performance of the MSSC algorithm, which is ideal so we are prepared for the large data rates envisaged with future VLBI observations.

*The current progress can be found here: `https://github.com/jradcliffe5/multi_self_cal_CASA.git`

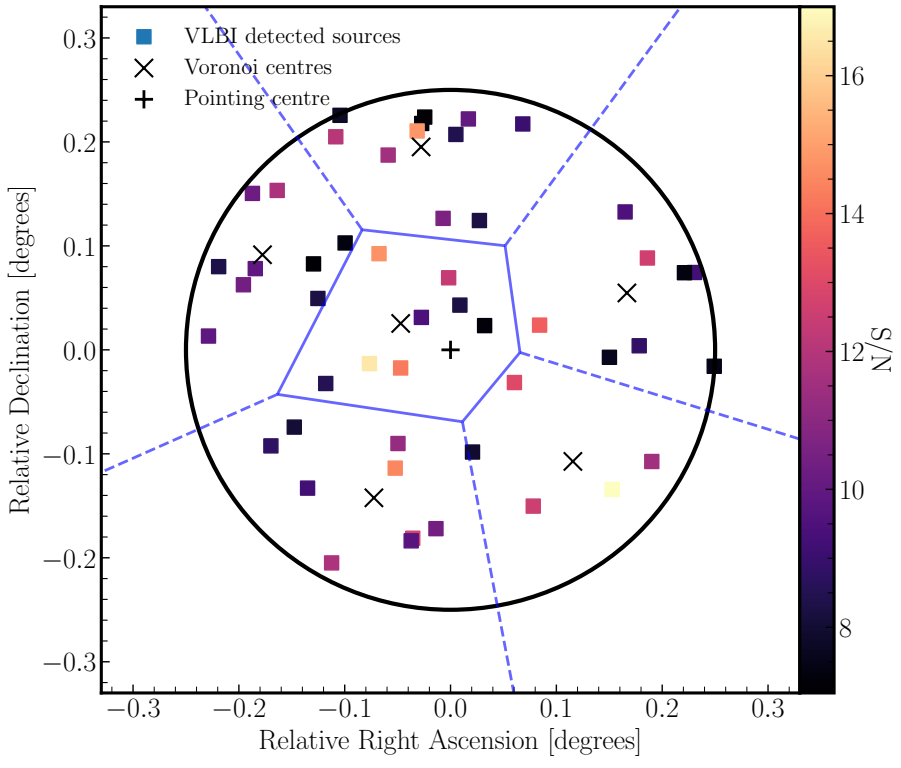

Figure 7.1 | An example of how MSSC can be used as a direction-dependent calibration technique within a wide-field VLBI observation using a single pointing. The bold black line corresponds to the FWHM of a 25 m parabolic dish at 1.4 GHz. Regions (blue solid and dashed lines) are partitioned such that the flux density within each Voronoi tile is identical. An independent phase solution can be derived for at the Voroni centre (black crosses) by performing MSSC on the sub-set of detected sources enclosed in the Voronoi region. These can be then applied to all the phase centres in the region.

The next version of MSSC aims to include full direction-dependent calibration support. While the existing standard MSSC algorithm provides an average correction for the phase-errors between the phase calibrator and target field, the phase variations across the primary beam of the VLBI array remain unsolved (unless manual sub-sets of VLBI sources are selected). The widening bandwidths, expanding VLBI arrays, the addition on sensitive elements (e.g. MeerKAT/SKA), and the improving surface brightness sensitivities of VLBI arrays means that the number density of VLBI sources is only going to increase in the future. Most importantly, the increased available S/N allows MSSC to automatically select sub-sets of VLBI sources and provide different phase solutions across the primary beam.

In Figure 7.1, we provide an example wide-field VLBI observation covering the entire FWHM of a 25 m parabolic antenna (~ 0.5 deg). Note that the underlying VLBI distribution is designed to be devoid of bright sources in order to simulate a faint target field. Weighted k-means clustering defines five separate regions that have comparable S/N ratios. The uv-stacking of sources in each region is sufficient to produce an average phase self-calibration solution at the Voronoi centres (black crosses). Assuming that the phase variations are slowly changing with respect to time, and there is sufficient S/N to separate the target field into multiple regions (ideally > 3) we can use an approach similar to the Multi-View algorithm, (Rioja et al., 2017) to improve dynamic range and astrometry of these observations. Here, the average phase solutions derived in each region can be interpolated across the entire FoV to produce a phase screen that can then be applied to all phase centres in the wide-field VLBI observation. This should provide the first truly direction-dependent calibration technique for wide-field VLBI observations.

7.2. VLBI-selected AGN in the microJy flux regime

While the VLBI observations presented here only reach a sensitivity of $9\mu\mathrm{Jy\,beam^{-1}}$, there is little knowledge about the nature of the VLBI-selected sources in the μJy flux density regime. The current deepest wide-field VLBI observations by Herrera Ruiz et al. (2018) reach an rms sensitivity of $\sim 3\,\mu\mathrm{Jy\,beam^{-1}}$. However, they only add an extra 10 sources to the 25 sources already detected in the previous observations (r.m.s. $\sim 10\,\mu\mathrm{Jy\,beam^{-1}}$).

Of particular interest is the evolution of the VLBI number counts. In Herrera Ruiz et al. (2018) they find that the number counts of VLBI-selected AGN match to the number counts of radio-selected AGN to flux densities of around $150\,\mu$Jy. They find that the VLBI selected number counts begin to drop off below this value. This could be due to the resolving out of flux in the VLBI observations, thus reducing the number of detections, or it could be due to a true shift in the AGN content of the persistent radio population.

To resolve this issue, we require larger and more sensitive samples of VLBI-selected sources. We shall achieve this using the final data release of the GOODS-N VLBI observations (estimated rms $\sim 2\,\mu\mathrm{Jy\,beam^{-1}}$), and the upcoming deep COSMOS observations using the EVN (PI: Radcliffe; estimated rms $\sim 1\,\mu\mathrm{Jy\,beam^{-1}}$). This will extend upon previous work, allowing the characterisation of VLBI-selected sources at the faintest flux density regime using a statistically significant sample.

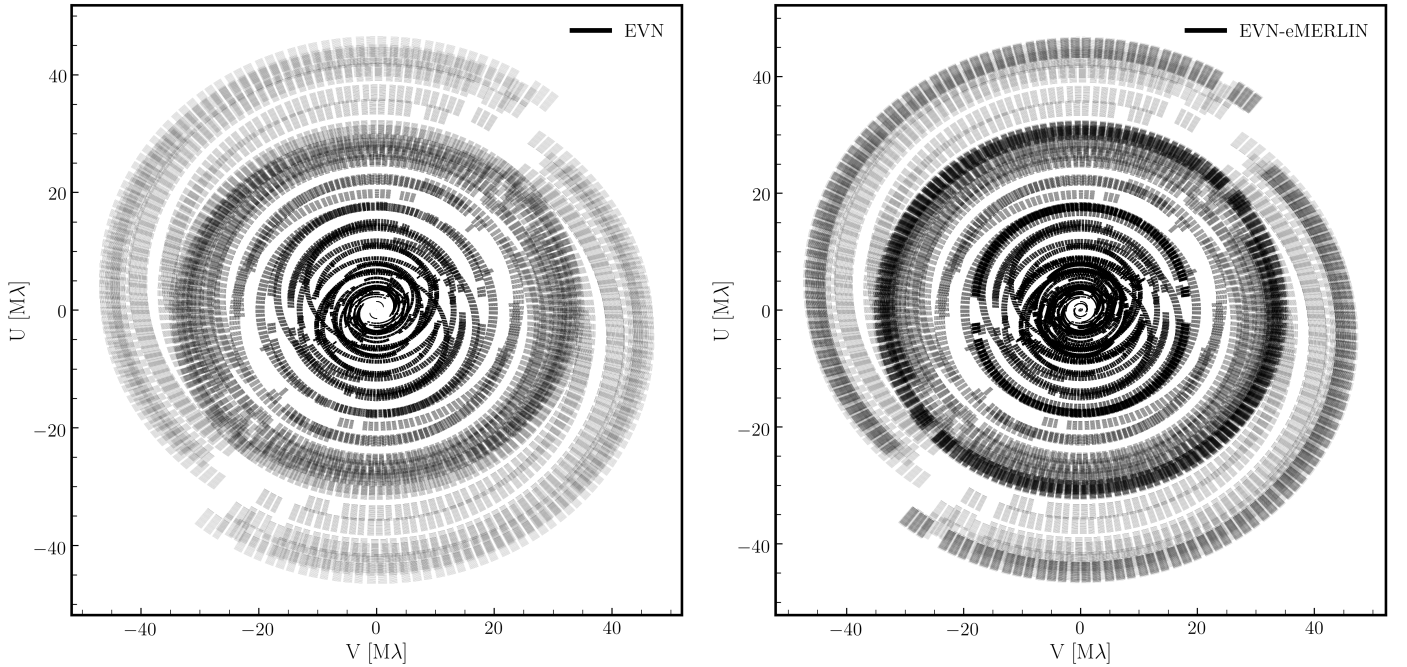

Figure 7.2 | The uv-coverage for the integrated EVN e-MERLIN observations of the GOODS-N field (EVN project code EG078G; Radcliffe et al. in prep.). The left panel shows the uv-coverage using just the telescopes of the EVN, while the right panel is for the entire array. The EVN-eMERLIN observations show a greater density of shorter spacings, thus permitting the characterisation of structure from the milliarcsecond to 0.2 arcsecond scales. The plot opacity corresponds to the density of uv points.

7.3. Identifying radio AGN for the MIGHTEE survey

As we outlined in chapter 4, the next generation of interferometers will conduct ultra deep surveys over large swathes of the sky. Many of these fields will not have deep multi-wavelength coverage required to identify contributions from AGN. In particular, the MeerKAT-MIGHTEE survey (Jarvis et al., 2016; Taylor & Jarvis, 2017), which acts as a precursor to the continuum studies with the SKA, will survey four of the most well-studied extragalactic deep fields. The survey will cover 20 square degrees to an r.m.s. sensitivity of $\sim 2\,\mu\mathrm{Jy\,beam^{-1}}$ sensitivity at GHz frequencies, including an ultra-deep image of a single 1 $\mathrm{deg^2}$ area. This survey will help us understand; 1) the evolution of AGN and star-formation activity over cosmic time free of dust obscuration; 2) the evolution of neutral hydrogen in the Universe and how this neutral gas eventually turns into stars after moving through the molecular phase, and how efficiently this can fuel AGN activity, and 3) the properties of cosmic magnetic fields and how they evolve in clusters, filaments and galaxies.

Whilst VLBI will not be able to detect the majority of the radiatively-efficient AGN, the varying sensitivity of the infra-red coverage in these fields means that radio-excess measurements cannot be evaluated for all sources. VLBI will prove vital in identifying a clean sample of compact radio-AGN in these systems. The EVN-COSMOS project along with the UDS VLBA project (PI: Deane) should provide this information whilst paving the way for a full scale MIGHTEE-VLBI project.

7.4. AGN feedback using integrated EVN and e-MERLIN observations

While this thesis has been mainly concerned with identifying AGN in distant galaxies, future work will attempt to investigate the role of AGN feedback within distant galaxies. Recent studies predict that AGN feedback must play a vital role in the evolution and formation of galaxies across cosmic time. Negative feedback, where the AGN 'quenches' star-formation, is popular amongst many and must play a role (e.g. Best et al., 2014), but its occurrence is not without doubt in populations of X-ray and radio-selected AGN (e.g. Harrison et al., 2012; Barthel et al., 2012).

We have secured integrated e-MERLIN and EVN observations for both the GOODS-N field and a new ultra-deep survey in the COSMOS field. The unique prospect of combined e-MERLIN and VLBI observations provides angular sensitivity over two orders of magnitude (~2-200 mas) within a single observation. In Figure 7.2, we illustrate the improvement in uv-coverage and therefore image fidelity, by comparing

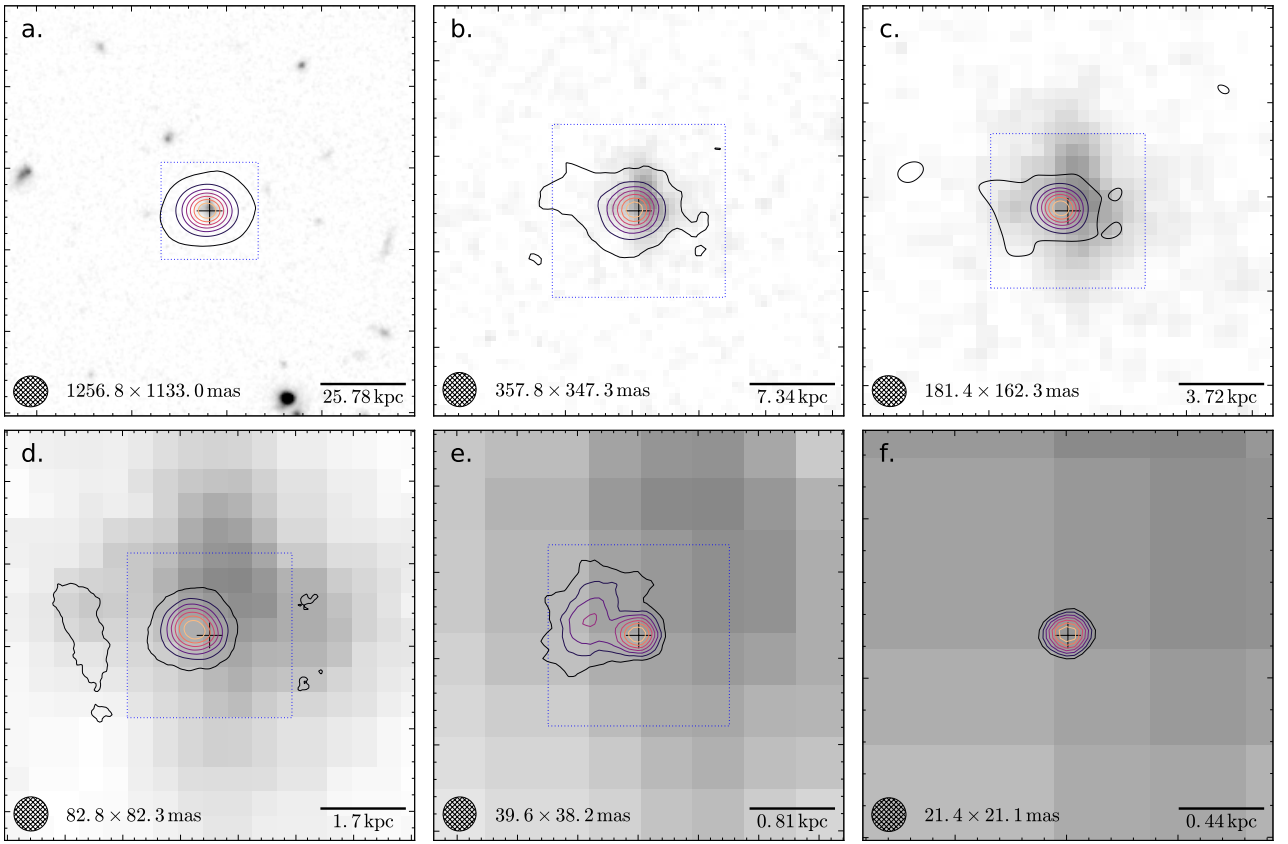

Figure 7.3 | J123642+621331 ($z \sim 2$), a composite star-burst ($\sim 100\,M_{\odot}yr^{-1}$ from its integrated IR flux) and AGN candidate, shown at increasingly higher resolutions. Magnification increases from a-f with the blue dotted outline indicating field-of-view of the subsequent image. The radio is overlaid on HST near-IR (F125W). The cross indicates the VLBI location of the AGN. The arcsecond to milliarcsecond resolutions, utilising a combination of VLA, e-MERLIN and EVN, reveal the existence of an AGN (Radcliffe et al. in prep.).

the EVN only and EVN-eMERLIN of the same observation of the GOODS-N field. The significant improvement of short spacings provides the vast angular resolution sensitivity.

The availability of multiple e-MERLIN telescopes within the EVN provides an essential component in order to probe the range of sub-kpc spatial scales required to enable not only a broad split of the μJy source counts into AGN and star formation-dominated sources, but a *genuine split of the AGN and star-formation contributions inside galaxies to this flux regime.*

For the GOODS-N field especially, this shall be enhanced further using VLA and e-MERLIN data from the **e-MER**lin **G**alaxy **E**volution (e-MERGE) survey. This supplementary data will increase the angular dynamic range sensitivity from the millarcsecond to arcsecond scales, permitting the first observations that will mimic the uv coverage that the SKA-2 will obtain. In Fig. 7.3, we show an example for the VLBI-detected source J123642+621331, which reveals the presence of a sub-jet using the combination of VLA, e-MERLIN and EVN data.

All together, this information will permit investigations into issues such as inside-out disk growth (e.g. Wang et al., 2011), spheroid/bulge formation (e.g. Nelson et al., 2016; Cibinel et al., 2017), and jet-induced star-formation (e.g. Gaibler et al., 2012).

7.5. SKA-VLBI

The Square Kilometre Array will be a revolutionary telescope and is expected to be three orders of magnitude more sensitive than current instruments. This improvement will allow further investigations into star-formation and AGN feedback across cosmic time, and allow us to investigate the radio emission of galaxies similar to our own at cosmological distances. Similarly to MeerKAT, not all of these observations will have coincident IR observations nor sufficient resolution to identify radio-emitting AGN. SKA-VLBI with angular resolutions $< 0\farcs01$, will therefore need to be utilised to provide the necessary angular resolution to isolate radio-AGN in large surveys. In Figure 7.4 we show the enhancement that the inclusion of VLBI has upon the angular resolution that can be obtained with the SKA. The techniques (e.g. primary beam correction and MSSC) and results from this thesis will be influential in the role of SKA-VLBI and the survey strategies adopted.

Bibliography

Barthel P., Haas M., Leipski C., Wilkes B., 2012, ApJ, 757, L26

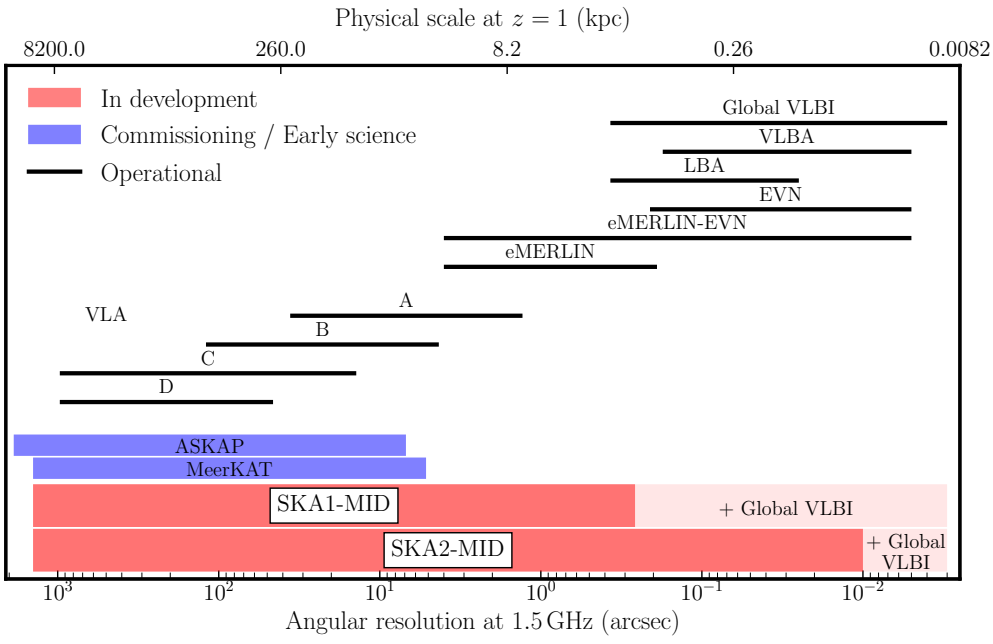

Figure 7.4 | The angular resolution at 1.5 GHz provided by the current suite of radio telescopes (black lines), the SKA-precursors (blue bars) and the SKA (red bars). The integration of VLBI into the SKA provides the extra resolution required to select compact radio-AGN in distant galaxies, as well as provide unrivalled sensitivity to a large range of angular scales.

7

Best P. N., Ker L. M., Simpson C., Rigby E. E., Sabater J., 2014, MNRAS, 445, 955
Cibinel A., et al., 2017, MNRAS, 469, 4683
Gaibler V., Khochfar S., Krause M., Silk J., 2012, MNRAS, 425, 438
Harrison C. M., et al., 2012, ApJ, 760, L15
Herrera Ruiz N., et al., 2018, A&A, 616, A128
Jarvis M., et al., 2016, in Proceedings of MeerKAT Science: On the Pathway to the SKA. 25-27 May. p. 6 (arXiv:1709.01901)
Nelson E. J., et al., 2016, ApJ, 828, 27
Rioja M. J., Dodson R., Orosz G., Imai H., Frey S., 2017, AJ, 153, 105
Taylor A. R., Jarvis M., 2017, IOP Conference Series: Materials Science and Engineering, 198, 012014
Wang J., et al., 2011, MNRAS, 412, 1081